

Deposition Modeling Updates for a Vertical System

Spent Fuel and Waste Disposition

***Prepared for
U.S. Department of Energy
Spent Fuel and Waste Science and
Technology***

Pacific Northwest National Laboratory

**SR Suffield
WA Perkins**

July 29, 2022
M4SF-22PN010207025
PNNL-33106

DISCLAIMER

This information was prepared as an account of work sponsored by an agency of the U.S. Government. Neither the U.S. Government nor any agency thereof, nor any of their employees, makes any warranty, expressed or implied, or assumes any legal liability or responsibility for the accuracy, completeness, or usefulness, of any information, apparatus, product, or process disclosed, or represents that its use would not infringe privately owned rights. References herein to any specific commercial product, process, or service by trade name, trade mark, manufacturer, or otherwise, does not necessarily constitute or imply its endorsement, recommendation, or favoring by the U.S. Government or any agency thereof. The views and opinions of authors expressed herein do not necessarily state or reflect those of the U.S. Government or any agency thereof.

SUMMARY

This report provides deposition modeling updates and results for a vertical spent nuclear fuel (SNF) storage system. The vertical storage system was NAC International's Modular, Advanced Generation, Nuclear All-purpose STORage System (MAGNASTOR®). The updates to the model included running a turbulence model sensitivity study and incorporating droplet evaporation into the deposition model for the MAGNASTOR®. In addition to the updates to the vertical MAGNASTOR® system this report discusses the topic of particle resuspension and suggests future work related to resuspension in both vertical and horizontal storage systems.

This page is intentionally left blank.

ACKNOWLEDGEMENTS

This work was conducted as part of the U.S. Department of Energy Spent Fuel and Waste Science and Technology campaign. The authors thank Ned Larson of the Department of Energy for his support and leadership in this research program. We would also like to thank our collaborators at Sandia National Laboratories. The authors would also like to thank our project management at Pacific Northwest National Lab, Brady Hanson and Steve Ross.

This page is intentionally left blank.

CONTENTS

SUMMARY	iii
ACKNOWLEDGEMENTS	v
ACRONYMS	xi
1. INTRODUCTION	1
2. TURBULENCE MODEL SENSITIVITY STUDY	3
2.1 Study with Simple Validation Model.....	3
2.1.1 Model Description.....	3
2.1.2 Turbulence Model Sensitivity Study.....	4
2.1.3 Meshing Study	4
2.1.4 Results.....	6
2.2 Study with Vertical MAGNASTOR® Model.....	7
2.2.1 Meshing Study	7
2.2.2 Results.....	9
3. MULTIPHASE MODEL.....	11
3.1 Model Description.....	11
3.2 Multiphase vs Non-Multiphase Results	11
4. RESUSPENSION	13
5. CONCLUSIONS AND RECOMMENDATIONS	15
6. REFERENCES	17

This page is intentionally left blank.

FIGURES

Figure 2-1. Geometry and Mesh of Simple Turbulent Deposition Validation Model	3
Figure 2-2. Kolmogorov Scale and Taylor Micro Scale for Refined RANS Vertical Turbulent Pipe Mesh	5
Figure 2-3. Mesh Sensitivity Study for LES Near Surface Mesh	6
Figure 2-4. Turbulence Model Sensitivity Results for Vertical Turbulent Pipe Validation Model	7
Figure 2-5. Kolmogorov Scale and Taylor Micro Scale for Refined RANS MAGNASTOR® Mesh	8
Figure 2-6. Axial Cross-section of Mesh through the Center of the MAGNASTOR® Module for (a) RANS Model and (b) LES Model	9
Figure 2-7. Canister Deposition for (a) Steady State RANS and (b) LES Models	10
Figure 3-1. Total Particle Deposition within the Overpack for (a) Non-Multiphase Model and (b) Multiphase Model	12
Figure 4-1. Example of the theoretical relationship between a critical shear velocity and resuspension of particles of specific size (from Nasr et al., 2017). This example is for glass particles on a steel substrate.	14
Figure 4-2. Example of the relationship between particle resuspension and exposure time under several flow conditions (from Habchi et al., 2016).	14

TABLES

Table 2-1. GCI – Vertical Turbulent Pipe Validation Model 5

Table 2-2. GCI - MAGNASTOR® Model 8

Table 2-3. Resulting Canister Deposition for MAGNASTOR® Turbulence Sensitivity Study..... 9

Table 3-1. Vertical MAGNASTOR® Storage Model Deposition Results 11

ACRONYMS

CAD	computer-aided design
CDF	cumulative distribution function
CFD	computational fluid dynamics
CISCC	chloride-induced stress corrosion cracking
CPU	central processing unit
DES	detached eddy simulation
ISFSI	Independent Spent Fuel Storage Installation
LES	large eddy simulation
PNNL	Pacific Northwest National Laboratory
RANS	Reynolds-averaged Navier-Stokes
Re	Reynolds number
RH	relative humidity
SSA	sea-salt aerosols
SCC	stress corrosion cracking
SNF	spent nuclear fuel
SST	shear stress transport

This page is intentionally left blank.

DEPOSITION MODELING UPDATES FOR A VERTICAL SYSTEM

1. INTRODUCTION

Deposition models are being developed with the commercial computational fluid dynamics (CFD) software STAR-CCM+ (Siemens PLM Software 2021) to evaluate contaminant deposition on spent nuclear fuel (SNF) canisters. The primary contaminant of concern is chloride, which is dispersed in the atmosphere and then deposits onto the canisters. For the nuclear industry, the deposition of sea-salt aerosols (SSAs) onto the surface of dry storage canisters at an Independent Spent Fuel Storage Installation (ISFSI) is a concern. During dry storage, the primary degradation process is likely to be chloride-induced stress corrosion cracking (CISCC) at the heat-affected zones of the canister welds. It is known that stainless steel canisters are susceptible to CISCC; however, the rate of chloride deposition onto the canisters is poorly known, based on sparse field data from a small number of sites.

This report describes updates to a previously developed model for a vertical spent nuclear fuel (SNF) storage system (Jensen 2020a and 2020b). The vertical storage system was NAC International's Modular, Advanced Generation, Nuclear All-purpose STORAge System (MAGNASTOR®). The updates to the model included running a turbulence model sensitivity study. A simple validation model was set up to run a turbulence model sensitivity study before implementing into the larger vertical MAGNASTOR® model. The simple model provided comparisons against measured data and was much more computationally efficient than the larger SNF model, allowing for more runs in a shorter amount of time and determining the turbulence models to run with the SNF model.

The previously developed STAR-CCM+ deposition models assumed dry air for the external canister gas. In reality, there will be some amount of water vapor present in the air, represented by the relative humidity (RH). SSAs are known to change in density as they travel through the atmosphere by responding to changes in RH (i.e., absorb or shed water relative to humidity changes). A multiphase model with air and water vapor accounting for RH was incorporated into the STAR-CCM+ MAGNASTOR® deposition model. In addition to adding water vapor to the environment, a droplet evaporation model was also added to the STAR-CCM+ deposition model.

In addition to the updates to the vertical MAGNASTOR® system this report discusses the topic of particle resuspension and suggests future work related to looking at resuspension in both a vertical and horizontal storage system.

This page is intentionally left blank.

2. TURBULENCE MODEL SENSITIVITY STUDY

Two turbulence model sensitivity studies were performed and are described in this section, a simple validation model and the MAGNASTOR[®] model. Both models had been constructed using the commercial software STAR-CCM+ (Siemens PLM Software 2021).

2.1 Study with Simple Validation Model

A simple validation model was built to simulate an experiment by Liu and Agarwal (1974). The experiment evaluated the deposition rate of aerosol particles in turbulent flow in a vertical straight pipe. The aerosol particles used in the experiment were uniform spherical droplets of olive oil containing a florescent tracer that was less than 10% by weight. The amount of tracer deposited on the walls was measured along a 102 cm long glass tube. The tube had a 1.27 cm inner diameter.

2.1.1 Model Description

A STAR-CCM+ model was constructed to simulate the experiment. The initial model was built using a k-omega shear stress transport (SST) turbulence flow model (Menter, 1994). The k-omega SST model uses the Reynolds-averaged Navier-Stokes (RANS) equations to solve for the fluid flow. The initial model was also run with a steady state solver.

A simple geometry of the air flowing through the vertical pipe was constructed in SolidWorks (Dassault Systemes SolidWorks Corp., 2021). The computer-aided design (CAD) geometry was imported into STAR-CCM+ and meshed. A 0.1 cm thick prism layer boundary with 20 cell layers was applied along the inner wall of the pipe. This ensured a wall y^+ value of less than 1 along the wall. The y^+ value represents the non-dimensional distance between the surface and height of the cell in contact with the surface, and a value of less than 1 ensures a fine mesh along surface. A radial cross-section of the mesh, taken through the center of the vertical pipe, is shown in Figure 2-1.

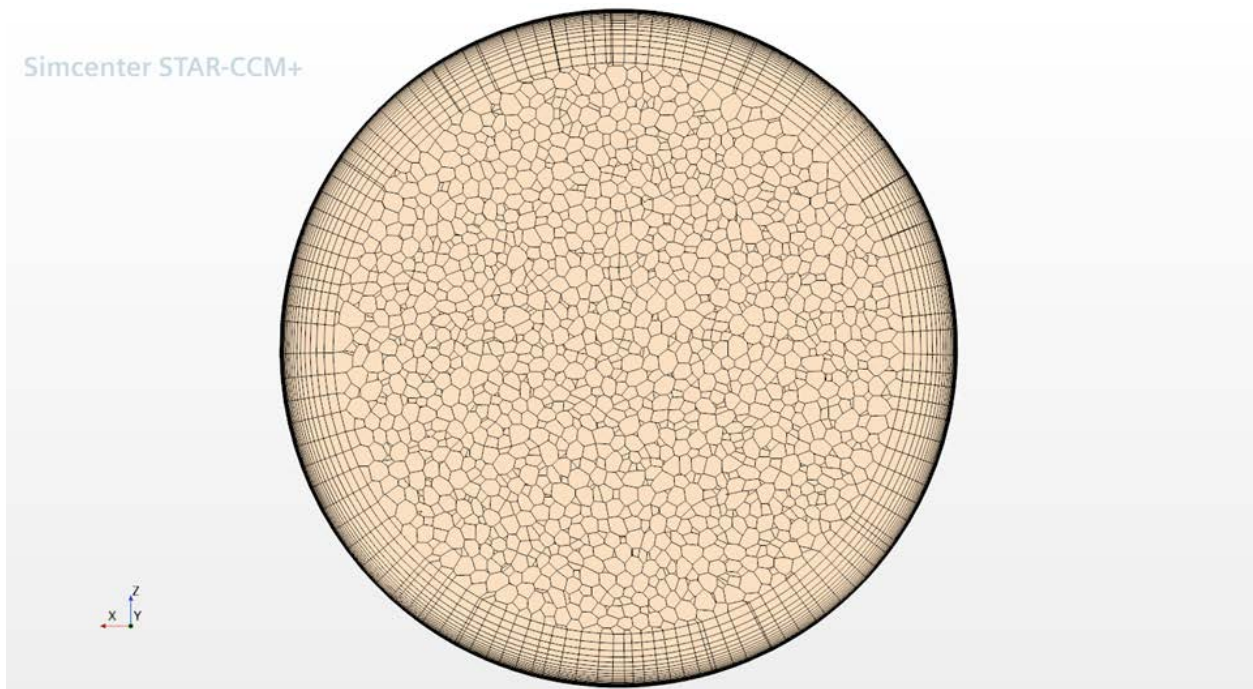


Figure 2-1. Geometry and Mesh of Simple Turbulent Deposition Validation Model

Deposition was evaluated from 12.75 cm to 63.75 cm, with 0 cm corresponding to the bottom of the pipe, to match the region measured and reported in the experiment (Liu and Agarwal 1974). The model was run at Reynold numbers (Re) of 10,000 and 50,000, and with different particle diameters ranging from 1.4-21 μm to match test conditions run by Liu and Agarwal (1974). A total of 5000 particles were injected at the tube inlet of the model.

2.1.2 Turbulence Model Sensitivity Study

A sensitivity study was set up to look at steady state and transient cases for various turbulence models. These turbulence models included a steady state RANS, a transient RANS, a transient Detached Eddy Simulation (DES), and a transient Large Eddy Simulation (LES). Our current deposition models use steady state RANS. The advantage of LES models for simulating inherently transient flows is that the large scales of turbulence are directly resolved in the flow domain and the small-scale motions are modeled. This leads to less error in the turbulence modeling by explicitly solving for more of those flow features (Siemens PLM Software 2021). The tradeoff is computational time. The mesh must be appropriate for the turbulence model. For LES, the mesh must be sufficiently small to allow the resolution of at least the largest turbulent eddies. A sufficiently meshed LES model for a SNF storage system could be challenging from a computational resources standpoint. The DES model combines features of the RANS model in the boundary layers with a LES in unsteady separated regions. The vertical turbulent pipe validation model was run with the various turbulence models for a Re of 50,000. The transient RANS case was run with a timestep small enough to ensure an average convective Courant number of less than 1 and a maximum convective Courant number of 50. The DES and LES transients were run with smaller timesteps to ensure that the maximum convective Courant number was less than 1.

2.1.3 Meshing Study

A mesh sensitivity study was performed on the vertical turbulent pipe validation model to ensure that the mesh was sufficiently resolved for the default steady state RANS model. The mesh sensitivity runs used a Re of 10,000 and a particle diameter of 21 μm . Three different resolutions of mesh were generated. An estimate of discretization error can be obtained by determining the Grid Convergence Index (GCI). This parameter is calculated following the approach outlined by Oberkampf and Roy (2010). The GCI is given by:

$$GCI = \frac{F_s}{r^{p-1}} \left| \frac{f_2 - f_1}{f_1} \right| \quad (1)$$

where;

F_s = is the factor of safety, equal to 1.25 for this calculation,

r = the grid refinement factor,

p = the order, which is 2 for these cases,

f = the solution for the cases, with f_1 designating the fine mesh solution and f_2 the solution for the coarse mesh.

The grid refinement ratio can be computed as:

$$effective\ r = \left(\frac{N_1}{N_2} \right)^{1/D} \quad (2)$$

where N_1 and N_2 are the total cell count for the fine and course meshes, respectively, and D is the dimensionality of the system. Applying this for the cell counts of the different mesh resolutions and resulting particle fraction removed shown in Table 2-1 yields the two estimates of GCI as shown in Table 2-1. Note that the GCI is not a bounding error estimate, rather an indication of the relative error. The refined mesh is used going forward for the vertical turbulent pipe validation model for the RANS turbulence models.

Table 2-1. GCI – Vertical Turbulent Pipe Validation Model

Model	# Cells	Particle Fraction Removed	GCI	Relative Error
Coarse	921,583	0.332	0.0998	0.0331
Refined	3,000,844	0.537	0.0004	0.0002
Very Refined	12,860,023	0.538	-	-

The refined RANS model was also used to estimate the grid resolution required for the LES simulation. LES requires a much finer mesh resolution than that for a standard k-omega RANS simulation. If the local grid size is too coarse the LES subgrid scale model will be employed for inappropriate length scales resulting in inaccurate results. Looking at the Kolmogorov Scale and Taylor Scale for the refined RANS mesh provides a reasonable estimate of the local cell size needed for LES (Siemens PLM Software 2021):

$$\text{Kolmogorov Scale} < \text{Cell Size} < \text{Taylor Scale}$$

Figure 2-2 shows plots of the Kolmogorov Length Scale and Taylor Micro Scale for the refined RANS mesh.

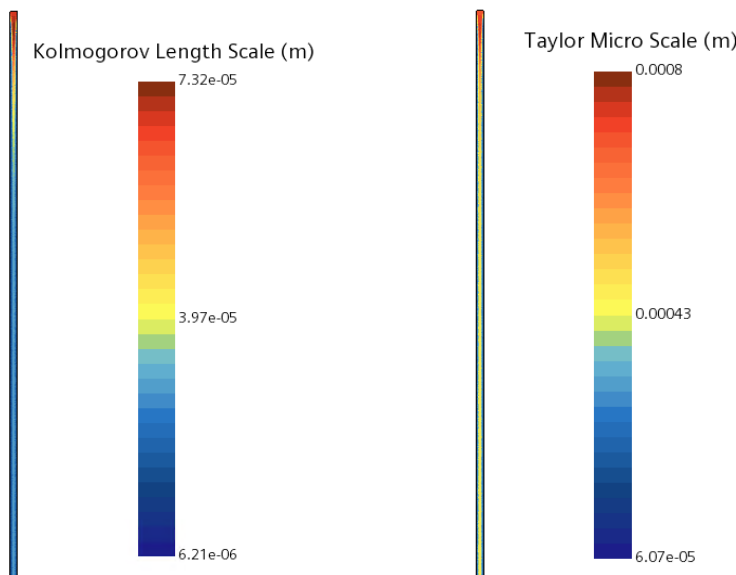


Figure 2-2. Kolmogorov Scale and Taylor Micro Scale for Refined RANS Vertical Turbulent Pipe Mesh

Based on the plots a target core mesh size of 0.75 mm was selected for the LES mesh. Ideally the mesh near the surface would have a target size of less than 6E-5 m (the minimum value from the Taylor Micro Scale plot) but this resulted in a very large model. A mesh sensitivity study was run varying the target surface size along the wall to determine the refinement needed for the LES model. Figure 2-3 shows the resulting particle deposition fraction for the mesh sensitivity study compared with the measured results from Liu & Agarwal (1974). The results show that the default RANS mesh greatly underestimates the particle deposition by predicting only 3% of 21 μm particles depositing on the wall of the tube versus 53% measured in the experiment. The refined mesh with a target surface size of 2.5E-4 m provided a

much better comparison with the measured data but slightly underpredicted deposition for the smaller particles. The refined mesh had a total number of 5,532,247 cells. The very refined mesh with a target surface size of $1.25E-4$ m provided the best comparison with the experiment data. It has a total number of 16,125,534 cells. The very refined mesh was used for the LES mesh in the turbulence model sensitivity study.

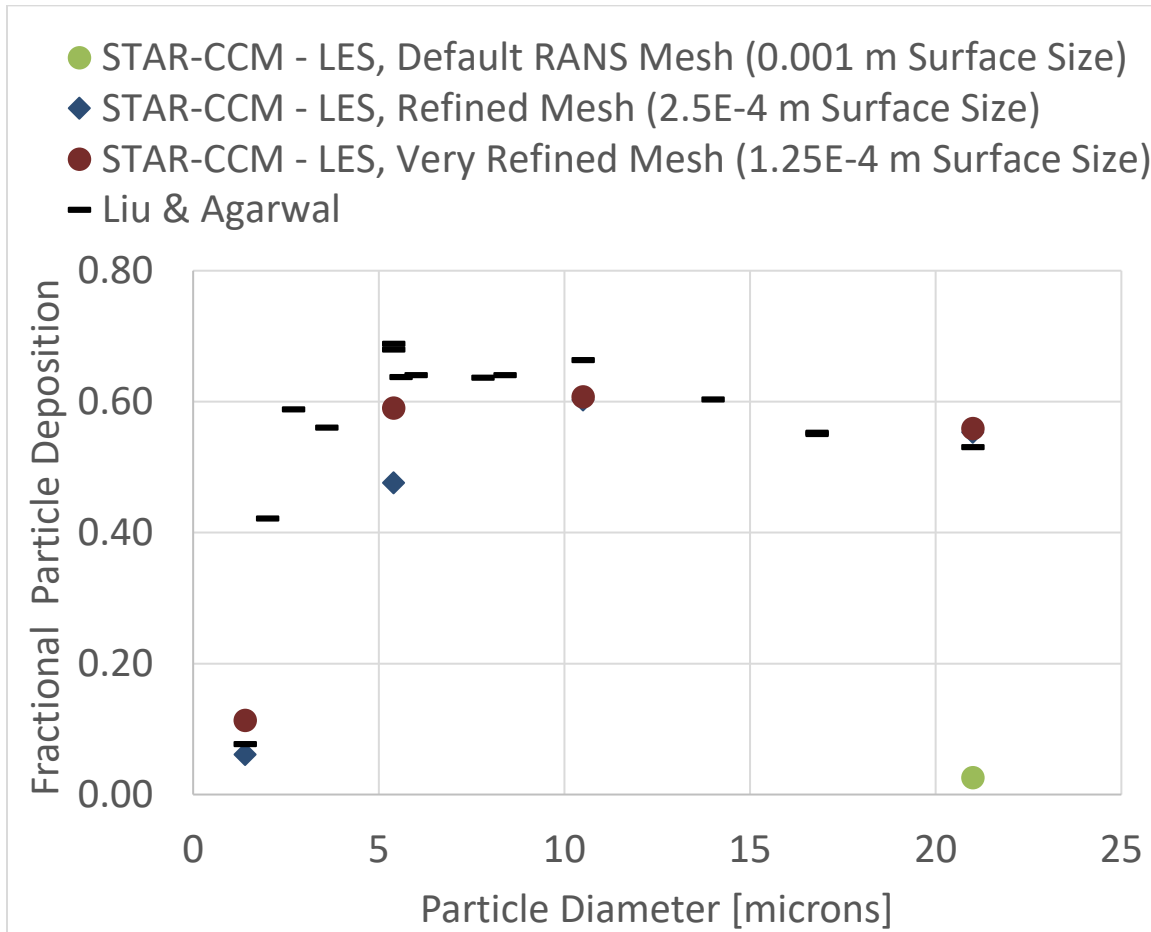


Figure 2-3. Mesh Sensitivity Study for LES Near Surface Mesh

The DES mesh was refined in the core mesh to a target size of 0.75 mm but kept the same near wall region mesh as the RANS model.

2.1.4 Results

The results from the turbulence sensitivity study are shown in Figure 2-4. All transient cases were run until the deposition was no longer changing with time. The results show that the steady state and transient RANS cases gave very similar results. Both RANS cases overpredicted the particle deposition for smaller particles, less than $10\ \mu\text{m}$ in diameter, compared to the measured data from the experiment. For the $1.4\ \mu\text{m}$ particles the RANS cases predicted deposition to be $\sim 48\%$, 6x more than the 8% measured by the experiment. The DES case produced similar results to the RANS cases, indicating treatment of the near wall region is driving deposition. DES is a hybrid of RANS and LES, with LES used in the core region and RANS in the near wall boundary layer. The LES model most closely approximated the measured data for the smaller particles. All turbulence models compared well with the experimental data for the larger particles, greater than $10\ \mu\text{m}$ in diameter. For the turbulence sensitivity study in the larger SNF storage

system the RANS and LES models will be considered. The DES turbulence model gave similar results as the RANS model but was much more computationally expensive with a refined core mesh and smaller timestep.

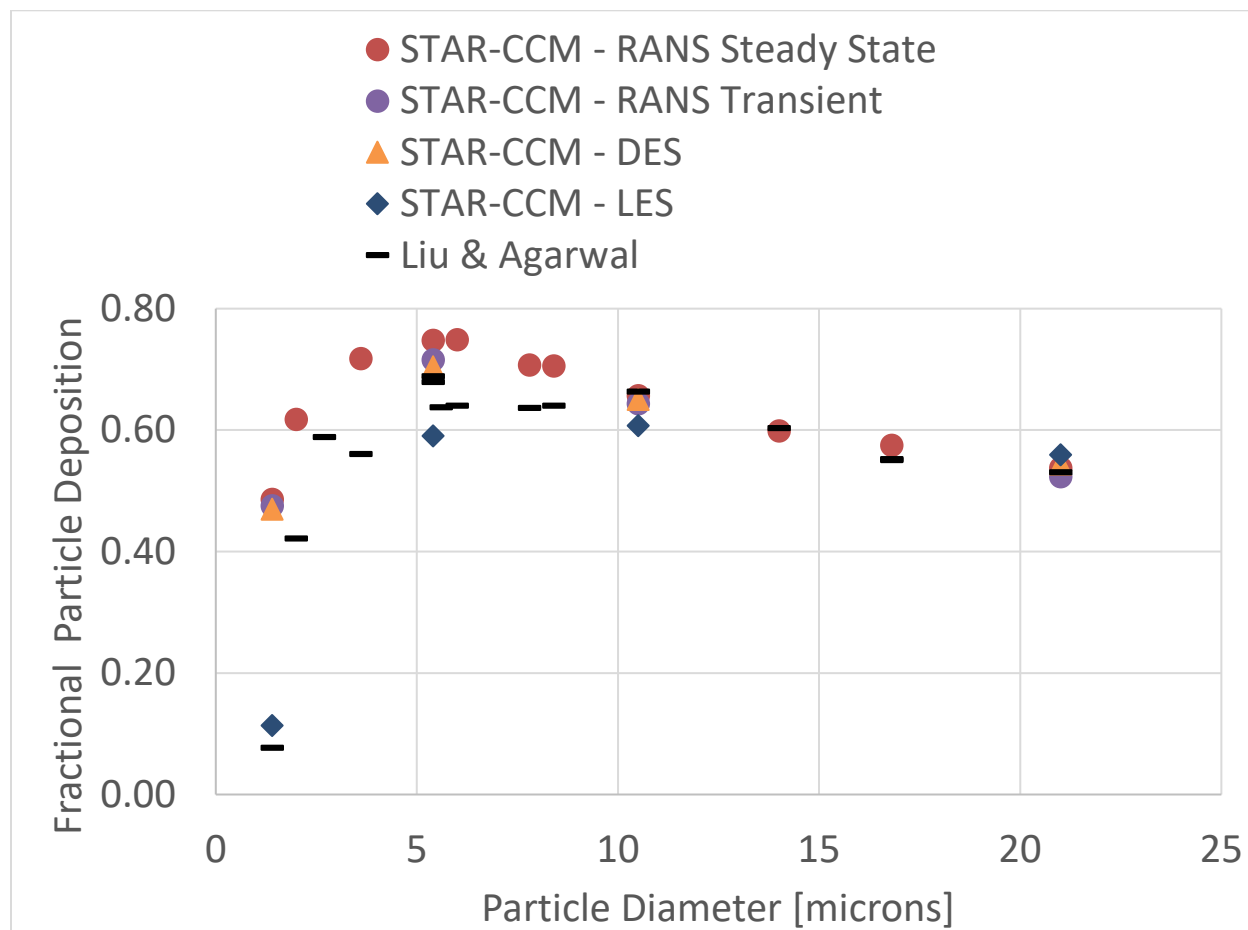


Figure 2-4. Turbulence Model Sensitivity Results for Vertical Turbulent Pipe Validation Model

2.2 Study with Vertical MAGNASTOR® Model

A detailed STAR-CCM+ thermal and deposition model was previously developed for the MAGNASTOR® storage system (Fort 2016, Jensen 2021). The MAGNASTOR® is a vertical storage system. A sensitivity study was set up to compare RANS and LES turbulence models. All models were run with a total heat load of 15 kW and an ambient temperature of 20°C. A uniform particle size distribution ranging from 0.25-25 μm was assumed for particles entering the inlets. The RANS turbulence models included a steady state and transient case. LES must be run as a transient model.

2.2.1 Meshing Study

A mesh sensitivity study was performed on the vertical MAGNASTOR® model to ensure that the mesh was sufficiently resolved for the default steady state RANS model. A GCI study as described in Section 2.1.3 was performed looking at maximum canister surface temperatures. The maximum canister

temperature was used for the GCI estimate since deposition will be dependent on canister surface temperatures. The results for the GCI are presented in Table 2-2. An estimate of the relative numerical error for the refined mesh solution is $0.0009 \times 175^\circ\text{C}$, which is 0.16°C . The refined mesh is used going forward for the MAGNASTOR[®] RANS models.

Table 2-2. GCI - MAGNASTOR[®] Model

Model	# Cells	Max Canister Temperature [°C]	GCI	Relative Error [°C]
Coarse	1947765	172.0	0.0061	1.05
Refined	5740113	175.0	0.0009	0.16
Very Refined	17422876	174.9	-	-

The refined RANS model was also used to estimate the grid resolution required for the LES simulation based on the Kolmogorov and Taylor Scale (as described in Section 2.1.3). Figure 2-5 shows plots of the Kolmogorov Length Scale and Taylor Micro Scale for the refined RANS mesh.

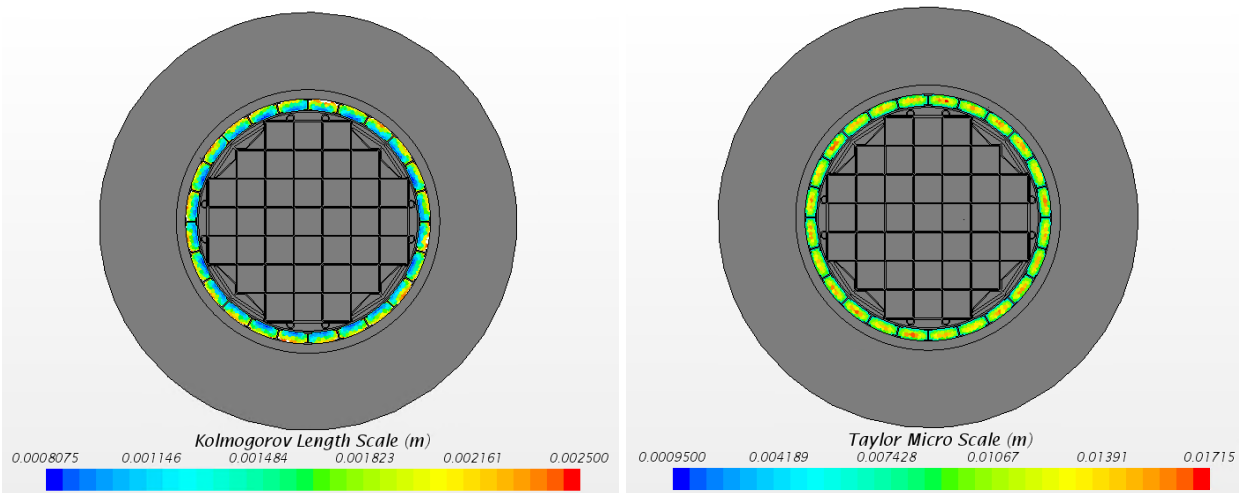


Figure 2-5. Kolmogorov Scale and Taylor Micro Scale for Refined RANS MAGNASTOR[®] Mesh

Based on the plots a target core mesh size of 0.015 m in the ventilated air region was implemented for the LES mesh. Ideally the mesh near the surface would have a target size of $\sim 9\text{E-}4$ m but this is not realistic for a large detailed SNF model such as the MAGNASTOR[®] model. The target surface cell size on the canister exterior was reduced to 0.01 m, which was a reduction factor of 2.5 from the refined RANS model. The resulting LES mesh had a total of 16,111,894 cells, 2.8 times larger than the refined RANS model. It is important to note that for computational efficiency only the canister surface was refined for the LES model since this is the primary surface of interest for deposition. An axial cross-section of the mesh for the RANS and LES model is shown in Figure 2-6.

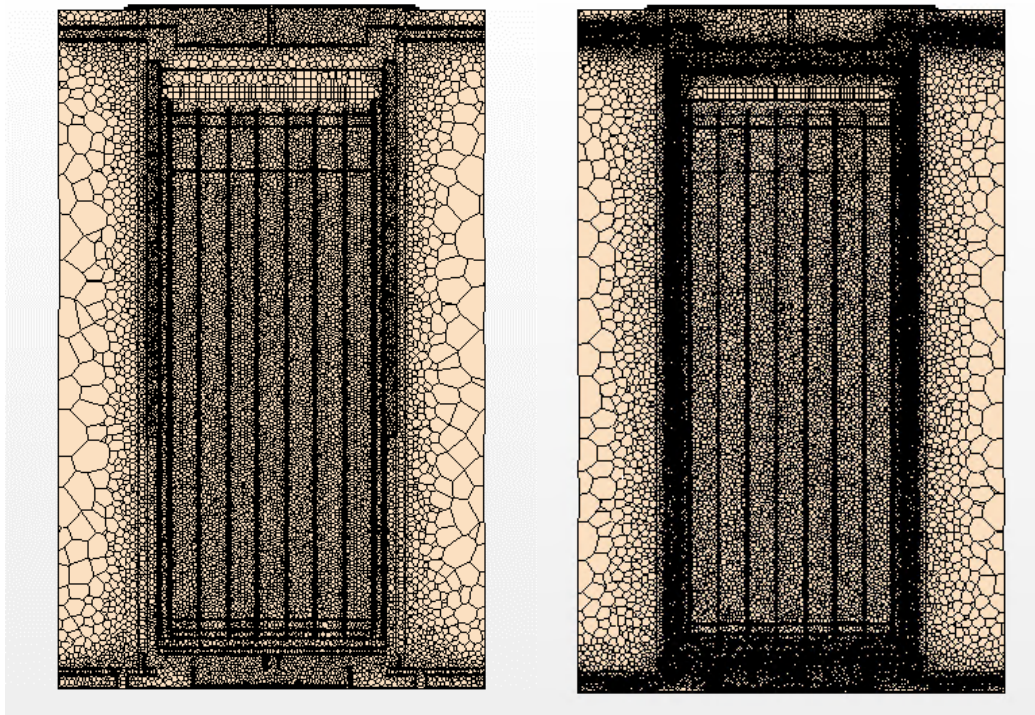


Figure 2-6. Axial Cross-section of Mesh through the Center of the MAGNASTOR® Module for (a) RANS Model and (b) LES Model

2.2.2 Results

All transient cases were run until canister deposition was no longer changing with time. To evaluate deposition, the canister deposition efficiency was calculated for each case. The deposition efficiency was calculated with the following equation:

$$\text{Deposition Efficiency} = \frac{\text{Mass of Stuck Particles}}{\text{Total Mass of Particles Entering Overpack}} \quad (3)$$

The results from the turbulence sensitivity study are shown in Table 2-3. All three cases gave very similar deposition results, with all models within 0.23% of each other. Table 2-3 also gives the total solver central processing unit (CPU) time for each case. The transient RANS cases required 31 times more CPU time compared to the steady state run, while the LES case required 120 times more CPU time. The results indicate that the default steady state RANS deposition models provide a reasonable estimate for deposition at a significantly lower computational expense.

Table 2-3. Resulting Canister Deposition for MAGNASTOR® Turbulence Sensitivity Study

Model	Canister Deposition Efficiency	Total Solver CPU Time [hrs]
MAGNASTOR® - Steady State RANS	2.66%	154
MAGNASTOR® - Transient RANS	2.73%	4,822
MAGNASTOR® - Transient LES	2.89%	18,484

The canister deposition is shown in Figure 2-7 for the steady state RANS and LES turbulence models. Both models show significantly more deposition along the top of the canister, which has also been noted in the visual inspection reports for the vertical canisters at Diablo Canyon (EPRI 2016). The LES model does show slightly more deposition along the sides of the canister.

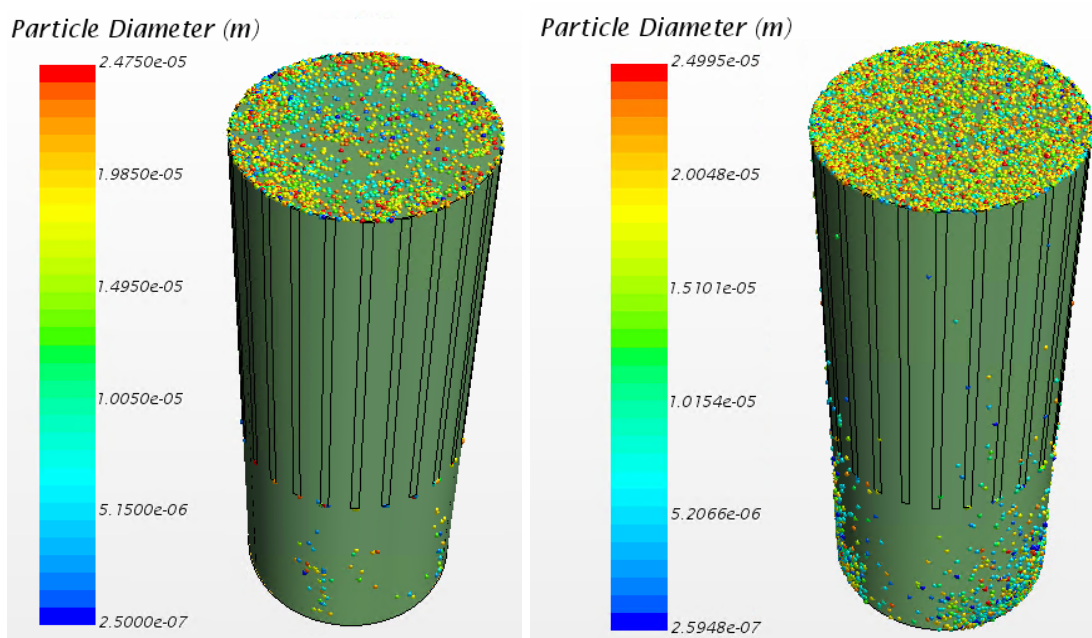


Figure 2-7. Canister Deposition for (a) Steady State RANS and (b) LES Models

3. MULTIPHASE MODEL

A multiphase model with air and water vapor accounting for the RH within the air was incorporated into the STAR-CCM+ deposition model for a vertical storage system. In addition to adding water vapor to the environment, a droplet evaporation model was also added to the STAR-CCM+ deposition model.

3.1 Model Description

The previously developed CFD model of the MAGNASTOR[®] vertical storage system (Fort 2016, Jensen 2021) was updated to a multiphase model with droplet evaporation. A multicomponent liquid representing a SSA particle made up of water and NaCl was incorporated into the MAGNASTOR[®] model. The previous model had assumed a simple solid particle. Water vapor was also incorporated into the ventilated air. The initial droplet composition assumed a solid mass fraction of 3.5% based on the salinity of ocean water (Zakowski 2014).

Steady state simulations were run with the MAGNASTOR[®] model with both the multiphase and non-multiphase model. The simulations assumed an ambient temperature of 20°C (68°F), RH of 78%, heat load of 15 kW, and a uniform particle size distribution from 0.25-25 µm for particles entering the overpack. Deposition was evaluated by calculating the deposition efficiency for each steady state run. The deposition efficiency equation given in Section 2.2.2 was based on particle mass but for the multiphase model the droplet mass will be changing as it moves through the heated overpack. For this reason, deposition efficiency was instead calculated based on particle counts:

$$\text{Deposition Efficiency} = \frac{\text{Stuck Particles}}{\text{Total Particles Entering Inlets}} \quad (4)$$

The model currently assumes a very simple “stuck” surface condition where if the particle makes contact with the surface, it is indefinitely stuck to the surface.

3.2 Multiphase vs Non-Multiphase Results

The resulting particle deposition for the multiphase and non-multiphase models are shown in Table 3-1. Total deposition within the overpack for the non-multiphase and multiphase model is plotted in Figure 3-1. The results show that with the multiphase model the total particle deposition in the overpack is less. This is likely due to smaller droplets traveling through the overpack due to droplet evaporation resulting in less settling of heavier particles. The results also show a slight decrease in particles depositing on the canister for the multiphase model. This may be due to thermophoresis, which is a particle force accounted for in the model. Thermophoresis describes motion of an aerosol in the opposite direction of a temperature gradient, causing particles near the heated canister surface to move away from the canister instead of depositing. Smaller particles will be more susceptible to thermophoresis, leading to slightly less of the smaller evaporated particles depositing on the canister.

Table 3-1. Vertical MAGNASTOR[®] Storage Model Deposition Results

Model	Total Particle Deposition Efficiency	Canister Particle Deposition Efficiency
Non-Multiphase Model	34.7%	1.8%
Multiphase Model	21.2%	0.8%

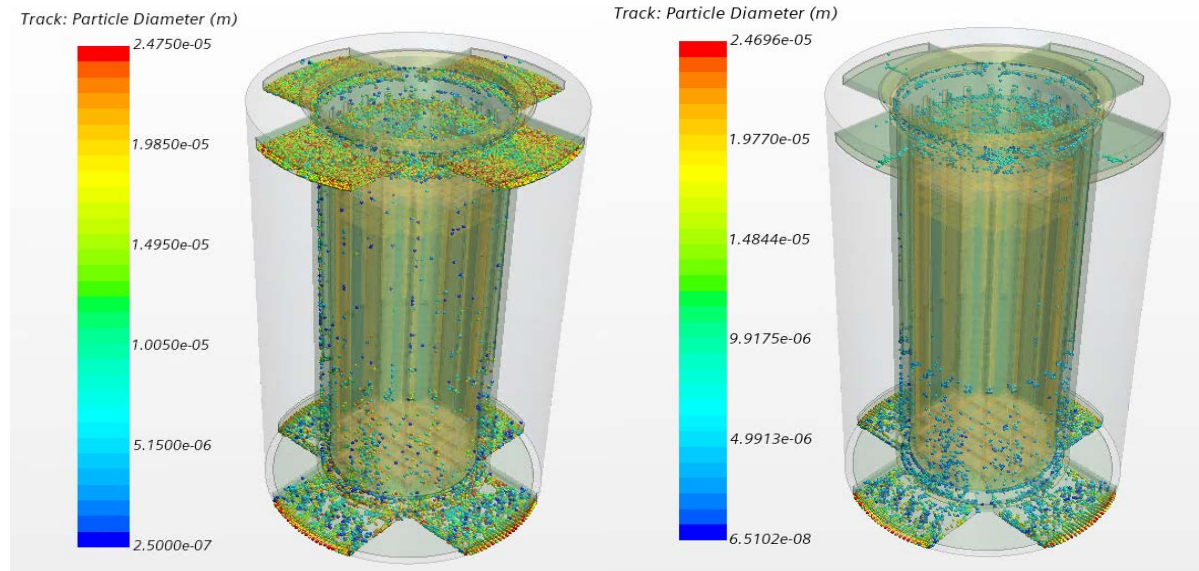


Figure 3-1. Total Particle Deposition within the Overpack for (a) Non-Multiphase Model and (b) Multiphase Model

4. RESUSPENSION

It might be assumed that SSA droplets would evaporate quickly once deposited on the heated canister surface leaving behind a chloride mass. It probably would be conservative to assume that this chloride would remain on cask surfaces and eventually contribute to CISCC; this is the “stuck” boundary condition described in the previous section. It is possible, however, that fluid motion could remove some or all deposited chloride particles before they have an adverse effect. We plan to investigate the significance of such resuspension, in order to justify its inclusion or exclusion in future analyses.

The necessary first step would be to quantify properties of the SSA chloride source. This could be derived from estimates of SSA chloride concentration and assumed distribution of SSA droplet size (from Leeuw et al., 2000; Eijk et al., 2011; Jensen et al., 2017, e.g.). While a SSA droplet size will change as it travels, reacting to atmospheric humidity, the mass of chloride it carries would remain the same. From this, deposited chloride particle size and necessary physical properties would be estimated.

Particle resuspension physics is well summarized in the literature (e.g. Henry and Minier, 2014; Nasr et al., 2017). The removal of a particle from a substrate surface depends on a number of particle/surface interaction forces. In general, though, these interactions are boiled down to a critical shear velocity that resuspends a specific sized particle. An example of such a relationship from literature is shown in Figure 4-1 for glass particles on a steel substrate. For this work, such a relationship would be needed for chloride particles on stainless steel. Shear velocity on the canister surface can be directly extracted from the simulations described above. This could be used to map the canister surface areas where chloride particles of specific size are likely to be resuspended. It is necessary to cross compare with those areas where deposition is indicated. If deposition is very unlikely, then resuspension need not be considered. Such analysis will provide if and where on the cask surface resuspension is indicated.

It may also be useful to investigate the time resuspended chloride particles stay on the surface. In turbulent flow, shear velocity to which deposited particles are exposed is necessarily randomly distributed. Consequently, particle resuspension is also a random process. Following the work of Habchi et al. (2016), simulated near wall velocity and turbulence parameters could be combined to develop a distribution of resuspended mass as a function of flow field exposure time. An example from Habchi et al. (2016) is shown in Figure 4-2. This distribution would vary over the cask surface and could perhaps be used to estimate the time required to resuspend some or all deposited chloride particle.

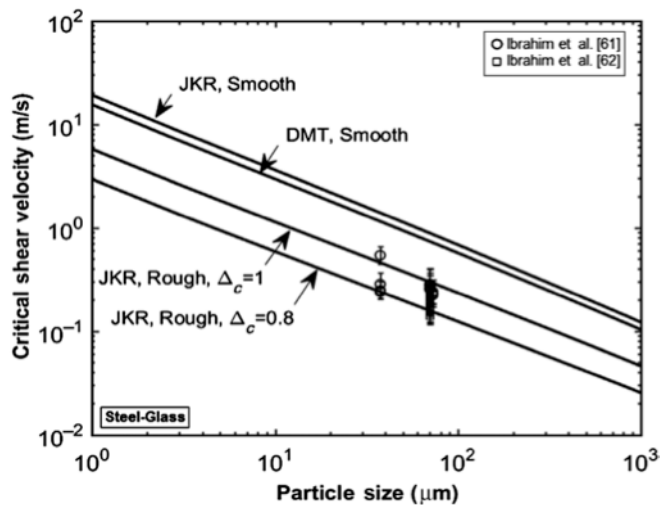


Figure 4-1. Example of the theoretical relationship between a critical shear velocity and resuspension of particles of specific size (from Nasr et al., 2017). This example is for glass particles on a steel substrate.

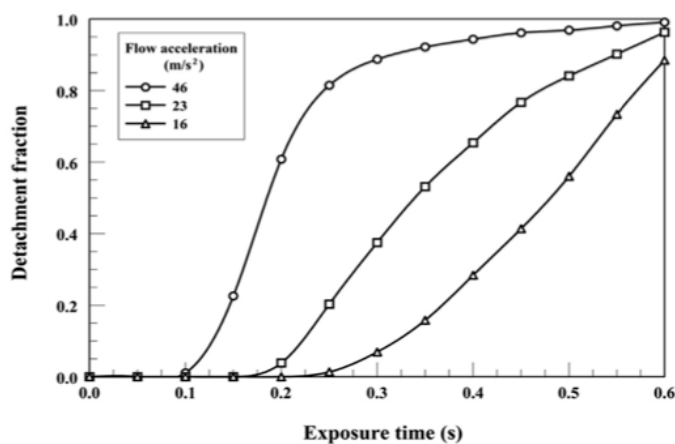


Figure 4-2. Example of the relationship between particle resuspension and exposure time under several flow conditions (from Habchi et al., 2016).

5. CONCLUSIONS AND RECOMMENDATIONS

This paper presents preliminary deposition results which includes updated models for a vertical system. A turbulence model sensitivity study was run with the MAGNASTOR[®] vertical system. The results show that the current RANS steady state models produce comparable canister deposition results as a much more computationally expensive LES model.

The MAGNASTOR[®] vertical system was also updated with a multiphase model that included adding water vapor to the ventilated air and droplet evaporation. The results showed that the addition of the multiphase model resulted in less overall deposition within the overpack and on the heated canister due to smaller droplets traveling through the overpack, resulting in differences in gravitational settling and thermophoretic particle forces.

The deposition models currently use a simple “stuck” boundary condition where if the particle makes contact with the surface, it is indefinitely stuck to the surface. Resuspension is currently being investigated. Potential approaches to investigating resuspension were summarized.

This work is a part of a larger effort, tasked with understanding the likelihood of canister degradation due to CISCC. These models are still under development and testing is needed for validation. However, these models are being presented now to demonstrate to canister vendors, utilities, regulators, and stakeholders the value of this type of modeling. This type of modeling could easily be adapted for their specific designs and sites.

This page is intentionally left blank.

6. REFERENCES

- Dassault Systemes SolidWorks Corp. 2021. SolidWorks Premium 2020 (computer software). Waltham, Massachusetts: Dassault Systemes.
- EPRI, *Diablo Canyon Stainless Steel Dry Storage Canister Inspection*. 2016, Electric Power Research Institute, Inc.
- J. D. Fontana (2011). Sea-spray aerosol particles generated in the surf zone. *Journal of Geophysical Research: Atmospheres* 116 (D19).
- Fort, J.A., T.E. Michener, S.R. Suffield, and D.J. Richmond. (2016). *Thermal Modeling of a Loaded Magnastor Storage System at Catawba Nuclear Station*. PNNL-25871: Pacific Northwest National Laboratories, Richland, Washington.
- Jensen, P., T. Tran, B. Fritz, F. Rutz, S. Ross, A. Gorton, R. Devanathan, P. Plante, and K. Trainor (2017, January). Preliminary Evaluation of the DUSTRAN Modeling Suite for Modeling Atmospheric Chloride Transport. *Air Quality, Atmosphere, & Health* 10(1), 25–31. Num Pages: 25-31 Place: Dordrecht, Netherlands Publisher: Springer Nature B.V.
- Jensen PJ, SR Suffield, CL Grant, CJ Spits, and JT Simmons. 2020a. *Preliminary Deposition Modeling: For Determining the Deposition of Corrosive Contaminants on SNF Canisters*. PNNL-29620. Pacific Northwest National Laboratory, Richland, Washington.
- Jensen PJ, SR Suffield, and BJ Jensen. 2020b. *Status Update: Deposition Modeling For SNF Canister CISCC*. PNNL-30793. Pacific Northwest National Laboratory, Richland, Washington.
- Jensen P.J., S.R. Suffield, C.L. Grant, C.J. Spitz, B.D. Hanson, S.B. Ross, and S. Durbin, et al. 2021. *Preliminary Modeling of Chloride Deposition on Spent Nuclear Fuel Canisters in Dry Storage Relevant to Stress Corrosion Cracking*. Nuclear Technology. PNNL-SA-156220. doi:10.1080/00295450.2021.1906086.
- Habchi, C., K. Ghali, and N. Ghaddar (2016, August). Coupling CFD and analytical modeling for investigation of monolayer particle resuspension by transient flows. *Building and Environment* 105, 1–12.
- Henry, C. and J.-P. Minier (2014, December). Progress in particle resuspension from rough surfaces by turbulent flows. *Progress in Energy and Combustion Science* 45, 1–53.
- Leeuw, G. D., F. P. Neele, M. Hill, M. H. Smith, and E. Vignati (2000). Production of sea spray aerosol in the surf zone. *Journal of Geophysical Research: Atmospheres* 105(D24), 29397–29409.
- Liu B and JK Agarwal. 1974. *Experimental Observation of Aerosol Deposition in Turbulent Flow*. Aerosol Science, 1974, Vol. 5. pp. 145-155.
- Menter FR. *Two-equation eddy-viscosity turbulence models for engineering applications*, AIAA J. 32 (1994) 1598–1605, <https://doi.org/10.2514/3.12149>.
- Nasr, B., S. Dhaniyala, and G. Ahmadi (2017, January). Chapter 2 - Particle Resuspension From Surfaces: Overview of Theoretical Models and Experimental Data. In R. Kohli and K. L. Mittal (Eds.), *Developments in Surface Contamination and Cleaning: Types of Contamination and Contamination Resources*, pp. 55–84. William Andrew Publishing.
- Oberkampf WL and CJ Roy. 2010. *Verification and Validation in Scientific Computing*. Cambridge University Press, New York.
- Siemens PLM Software. 2021. STAR-CCM+ 16.02 (computer software). Plano, Texas: Siemens PLM Software.
- Zakowski, K., A. Narozny, M. Szocinski, and K. Darowicki. Environ. *Influence of water salinity on corrosion risk – the case of the southern Baltic Sea coast*. Monit Assess. 2014. 186:4871-4879. DOI: 10.1007/s10661-014-3744-3.
-